Power loss reduction in the energy resource scheduling of a local energy community

Power Loss Reduction in the Energy Resource Scheduling of a Local Energy Community

Maria Maddalena Gambini
Dept. of Electrical, Electronic and Information Engineering
University of Bologna
Bologna, Italy
maria.gambini2@unibo.it

Camilo Orozco
Dept. of Electrical, Electronic and Information Engineering
University of Bologna
Bologna, Italy
camilo.orozco2@unibo.it

Alberto Borghetti
Dept. of Electrical, Electronic and Information Engineering
University of Bologna
Bologna, Italy
alberto.borghetti@unibo.it

Fabio Tossani
Dept. of Electrical, Electronic and Information Engineering
University of Bologna
Bologna, Italy
fabio.tossani@unibo.it

***Abstract*— The paper focuses on the minimization of the energy procurement cost in the day-ahead optimization of the operation of a local energy community. The community is a set of prosumers, each of them equipped with local generation, energy storage systems and loads. The procedure is based on the classical second order cone programming (SOCP) formulation of the distribution optimal power flow and distinguishes between the power exchanged with the external grid and the power exchanges between the prosumers in order to prioritize the use of local energy resources. The performance of the proposed procedure is shown for various operating conditions of a distribution network in which direct transactions between prosumers connected to different feeders of the same substation are allowed.**

Keywords*— *battery energy storage; energy scheduling; local energy community; renewable resources; second order cone programming.

NOMENCLATURE

Ω – set of prosumers and branches (index i)
r, x – branch resistance and reactance
T – set of scheduling periods t, each of duration Δt
v_{in} , v_{out} – square rms value of the input and output voltages
v_{min} , v_{max} – square values of the max and min voltage limits
u – square rms value of the branch current
P_{in} , P_{out} – input and output active power flows
Q_{in} , Q_{out} – input and output reactive power flows
P_{user} , Q_{user} – prosumer's net active and reactive power
P_l , Q_l – prosumer's active and reactive power consumption
P_g , Q_g – prosumer's active and reactive power generation
P_{BES} – prosumer's battery energy storage (BES) output
E – prosumer's BES energy level
ℓ_{charge} , $\ell_{discharge}$ – charge and discharge battery power losses
P_{grid} – prosumer's power exchanged with the external grid (P_{buy_grid} power bought at price π_{buy}, P_{sell_grid} power sold at price π_{sell}, P_{grid_in} and P_{grid_out} input and output power flows)

I. INTRODUCTION

This paper deals with a local energy community (LEC) composed of a set of medium voltage (MV) industrial/commercial/residential prosumers connected to the same or different feeders of the same primary substation. The aim of the community is to minimize the energy procurement cost by prioritizing the use of the internal resources with respect to the exchanges with the external network, as analyzed in [1],[2] and references therein. The economic justification is due to the difference between the price of the energy supplied by the external energy provider, identified with the utility grid for the sake of simplicity, and the price paid to a prosumer who sells power to the utility grid.

With the presence of renewables and storage units, the local energy community needs a day-ahead scheduling of the resources. For this purpose, various approaches have been proposed: [3],[4],[5] focus on peer-to-peer exchanges and the use of the block-chain technology, [6] presents a model of multiple distributed energy systems connected through a local grid and heating network, [7] proposes an agent-based approach to exploit generation/demand flexibility, [8] addresses the scalability issue of cooperative peer-to-peer energy sharing, [9] investigates the role of a community manager. The optimization problem gets harder to solve if power loss and typical operating constraints (such as bus voltage and branch current limits) are considered, e.g., [10] and references therein. We follow the classical second order cone programming (SOCP) formulation of the optimal power flow (OPF) in radial networks described in, e.g., [11], [12], considering the conditions to achieve exactness of the relaxation presented in [13], [14] and the analysis of topologies for which is not possible to guarantee the conditions for exactness as analyzed in [15].

To give priority to the use of internal energy resources, the formulation is extended to explicitly distinguish direct energy transactions between the prosumers from energy exchanges with the utility grid. The formulation is conceived so that it can be addressed by a distributed optimization procedure, although not presented in this paper. The performances of the procedure are illustrated for various operating conditions of a distribution network in which direct transactions between prosumers connected to different feeders of the same substation are allowed.

The structure of the paper is the following. Section II describes the model. Section III presents the comparison between the test results obtained with the proposed LEC model and the results obtained without allowing direct transactions between prosumers. Section IV concludes the paper.

II. THE MODEL

The model of the LEC is illustrated in Fig. 1. The internal network of the LEC, connected to the utility grid, is divided into elements corresponding to the prosumers. Each prosumer is characterized by a single connection point (coupling bus) to the network. The prosumer can inject or absorb power and incorporates the losses of the branch that connects its coupling bus with the coupling bus of the previous prosumer towards the substation. The attribution of the entire losses in each branch to the prosumer at the end of the branch is used only in

This work is supported in part by the European EIT Climate-KIC fund in the framework of the "Green Energy Community – GECO" project and by the European Union's Horizon 2020 research and innovation programme under the Marie Sklodowska-Curie grant agreement No 675318 (INCITE).

the scheduling optimization procedure, whilst the billing procedure implements a fair repartition of the branch losses to all the prosumers in the feeder, as the one described in [16] based on the readings of the LEC meter and the users' meters. This procedure is justified by the cooperative nature of the LEC, in which the prosumers are not in competition with each other but collaborate to achieve the common objective, i.e. the minimization of the community procurement costs.

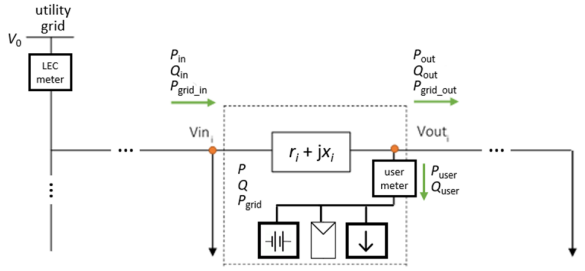

Fig. 1. Scheme of the LEC model. The green arrows indicate the positive directions assumed in the equations.

The mathematical formulation refers to a day-ahead scheduling, so the optimization horizon T is 24 h. The objective is

$$OF = \min \sum_{i\in\Omega} \sum_{t\in T} \left(\pi_{\text{buy},t} P_{\text{buy\_grid}\,i,t} - \pi_{\text{sell},t} P_{\text{sell\_grid}\,i,t} \right) \Delta t \quad (1)$$

where nonnegative variables $P_{\text{buy\_grid}\,i,t}$ and $P_{\text{sell\_grid}\,i,t}$ are the power bought from and sold to the utility grid by each prosumer i at time interval t, $\pi_{\text{buy},t}$ and $\pi_{\text{sell},t}$ are the profiles of the prices of buying and selling energy from and to the external utility grid, respectively assumed known for the next day. Since we assumed that all the local energy generation is provided by photovoltaic panels (PV), (1) does not include the costs of generation.

The objective minimizes the total procurement costs of the entire LEC. Since $\pi_{\text{buy},t}$ is higher than $\pi_{\text{sell},t}$, the objective penalizes the exchanges with the utility and favors the balance between production and consumption inside the LEC.

Fig. 1 illustrates the connection constraints between each branch (and the relevant prosumer) and the next one in the feeder, following the usual convention of the Distflow or branch flow model [17]: the values of v_{out}, P_{out}, Q_{out}, and $P_{\text{grid\_out}}$ of prosumer i are constrained to be equal to the values of v_{in}, P_{in}, Q_{in}, and $P_{\text{grid\_in}}$ of prosumer i+1. For the prosumers located at one of the feeder ends, P_{out}, Q_{out}, and $P_{\text{grid\_out}}$ are constrained to be 0. In case of branching, for active and reactive power the equality is replaced by the balancing constraints at the branching node, as in [17]. Values v_{in} of the branches connected to the substation (assumed to be the slack bus) are constrained to be the square of the known value of the slack bus voltage (V_0^2).

For each prosumer i and time interval t, the links between v_{in} and v_{out}, P_{in} and P_{out}, Q_{in} and Q_{out} are

$$P_{\text{in}\,i,t} - P_{\text{out}\,i,t} = P_{i,t} \quad (2)$$

$$Q_{\text{in}\,i,t} - Q_{\text{out}\,i,t} = Q_{i,t} \quad (3)$$

$$v_{\text{in}\,i,t} - v_{\text{out}\,i,t} = 2r_i \cdot P_{\text{in}\,i,t} + 2x_i \cdot Q_{\text{in}\,i,t} - (r_i^2 + x_i^2) \cdot u_{i,t} \quad (4)$$

$$P_{\text{in}\,i,t}^2 + Q_{\text{in}\,i,t}^2 \le v_{\text{in}\,i,t} \cdot u_{i,t} \quad (5)$$

where u, square of the rms value of the branch current, is constrained to be lower than the square of the maximum current limit, $P=P_{\text{user}}+r\cdot u$ and $Q= Q_{\text{user}}+x\cdot u$ include also the branch active and reactive power losses (shunt capacitances of the branches are neglected). Constraint (5) is the usual rotated second order cone convex relaxation of the branch flow model.

Considering that each prosumer has a generating unit and a storage unit, in addition to its load, net powers at the coupling bus are given by

$$P_{\text{user}\,i,t} = P_{1\,i,t} - P_{\text{g}\,i,t} - P_{\text{BES}\,i,t} \quad (6)$$

$$Q_{\text{user}\,i,t} = Q_{1\,i,t} - Q_{\text{g}\,i,t} \quad (7)$$

where P_{BES}, the power output of the storage unit, is considered positive if supplied by the battery. In this paper we assume that the PV units operate at the unity power factor (Q_{g}=0) and the power profile of loads and generators are equal to the corresponding forecasted values for the next day. P_{BES} is the main control variable together with the trade decisions with the other prosumers of the community as shown below.

The adopted simple model of the storage unit considers charging and discharging efficiencies (η_{charge} and $\eta_{\text{discharge}}$):

$$P_{\text{BES}\,i,t} = P_{\text{BES}\,i,t}^{+} - P_{\text{BES}\,i,t}^{-} \quad (8)$$

$$\ell_{\text{charge}\,i,t} = (1 - \eta_{\text{charge}\,i}) P_{BES\,i,t}^{-} \quad (9)$$

$$\ell_{\text{discharge}\,i,t} = (1/\eta_{\text{discharge}\,i} - 1) P_{BES\,i,t}^{+} \quad (10)$$

were both P_{BES}^{+} and P_{BES}^{-} are nonnegative variables constrained by the maximum power limit of the battery. The energy level E inside each battery is constrained to be between 10% and 100% of the battery rating and is calculated by

$$E_{i,t} = E_{i,t-1} - (P_{\text{BES}\,i,t} + \ell_{\text{charge}\,i,t} + \ell_{\text{discharge}\,i,t}) \Delta t \quad (11)$$

In the simulations we assume that the energy level at the beginning of the first interval and at the end of the optimization horizon are constrained to be equal to the battery rating.

The direct exchanges with the utility grid are described by variable P_{grid} (and the corresponding variables at the boundaries, namely $P_{\text{grid\_in}}$, and $P_{\text{grid\_out}}$):

$$P_{\text{grid}\,i,t} = P_{\text{buy\_grid}\,i,t} - P_{\text{sell\_grid}\,i,t} \quad (12)$$

$$P_{\text{grid\_in}\,i,t} - P_{\text{grid\_out}\,i,t} = P_{\text{grid}\,i,t} \quad (13)$$

$$P_{i,t} = P_{i,t}^{+} - P_{i,t}^{-} \quad (14)$$

$$\left| P_{i,t} \right| = P_{i,t}^{+} + P_{i,t}^{-} \quad (15)$$

where nonnegative variables P^+ and P^- defined by (14) and (15) are used to constrain nonnegative variables $P_{\text{buy\_grid}}$ and $P_{\text{sell\_grid}}$, respectively: $P_{\text{buy\_grid}} \le P^+$ and $P_{\text{sell\_grid}} \le P^-$.

For each prosumer i and time interval t, the transactions inside the community are calculated by the difference between P and P_{grid}: $P^+ - P_{\text{buy\_grid}}$ is the power bought from other prosumers, $P^- - P_{\text{sell\_grid}}$ is the power sold to other prosumers. The modulus of the dual values associated to constraints (13) are used as the prices for the transactions between prosumers inside the LEC.

The following constraint allows exchanges between different feeders connected to the same substation:

$$\sum_{k\in\Omega_0} P_{\text{grid\_in}\,k,t} = \sum_{k\in\Omega_0} P_{\text{in}\,k,t} \qquad (16)$$

where Ω_0 is the set of branches connected to the slack bus.

In a feasible solution, (5) is verified as an equality and, powers P^+_{BES} and P^-_{BES} of (8) can never be different from zero simultaneously for the same prosumer. Specific checks are included in the implementation of the model and additional penalization terms are added to (1), with increasing weights if needed. For each *i* and *t*, the penalization term relevant to (5) is $r \cdot u$ (branch power loss) and the penalization term for the battery model is $\ell_{\text{charge}} + \ell_{\text{discharge}}$ (losses in the storage unit). For the test cases considered in this paper, the penalization terms are negligible with respect to the cost terms shown in (1).

In summary, the optimization problem is composed by objective function (1), augmented with the above mentioned terms to guarantee the feasibility of the solution, constraints (2)-(16), and the lower and upper limits of each variable.

III. Test Results

The model has been implemented in Matlab and tested by using the Gurobi 9.0 solver (MIQCP model) on an Intel-i7 computer with 8 GB of RAM, running 64-bit Windows 10. The one-day horizon is divided into 24 periods of one hour each.

The test system is the 14-bus network with three feeders shown in Fig. 2, adapted from [18]. The MV side of the substation has constant rated voltage V_0=23 kV. All the other 13 buses are represented by PQ nodes. The power factor at each node and the resistance and reactance values are those indicated in [18]. Each prosumer is equipped with a PV system, a load, and a BES unit.

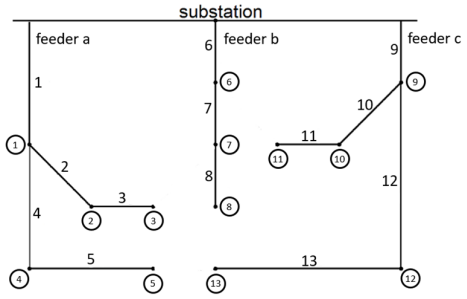

Fig. 2. Test system configuration. Circles indicate the location of the prosumers.

A. Base case operating condition

In the operating condition considered as base case, the total daily consumption of the LEC is 195 MWh and the corresponding PV production is 56 MWh (28.7% of the load). The load profiles adopted for each prosumer are shown in Fig. 3 (the inputs of the model are the average values in each hour). For all the PV units we assume the same profile of the ratio between power output and panel surface, also shown in Fig. 3, but a different PV surface for each prosumer as shown in TABLE I. The sizes of the BES units are shown in TABLE II with energy to power ratio equal to 1 h. The total capacity of the BES units is 5.5 MWh (9.8% of the daily PV production).

The load and PV production are differently distributed in the three feeders. In feeder a, the total daily consumption is 82 MWh, the PV production is 36.4 MWh (18.6% of the load), and the total BES capacity is 1.7 MWh (4.7% of PV production). In feeder b, the total daily consumption is 79 MWh, the PV production is 0, and the total BES capacity is 2.5MWh. In feeder c, the total daily consumption is 34 MWh, the PV production is 10 MWh (10.1% of the load), and the total BES capacity is 1.3 MWh (6.6% of PV production).

Fig. 4 shows the price profile of the energy bought from the utility grid π_{buy} and the price of the energy sold by the LEC to the utility grid π_{sell} (assumed half of π_{buy}).

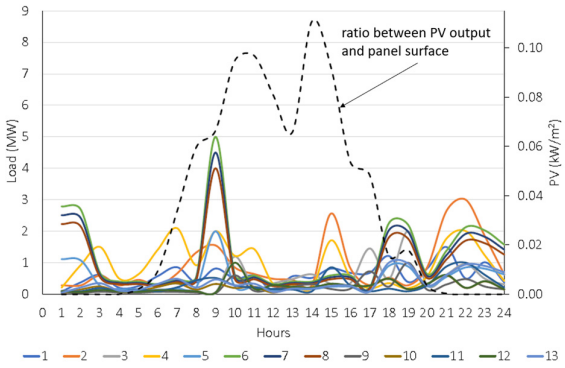

Fig. 3. Load profile for each prosumer and PV production per m^2.

TABLE I PV surface for each prosumer (in 10^3 m^2).

user	1	2	3	4	5	9	10	11	12	13
size	1.12	2.56	11.2	25.6	2.24	6.72	5.12	4.48	3.36	3.36

TABLE II Sizes of the BES units (in MWh).

user	1	2	3	4	5	6	7	8	9	10	11	12	13
size	0.5	0.3	0.4	0.2	0.3	1	0.5	1	0.2	0.6	0.1	0.2	0.2

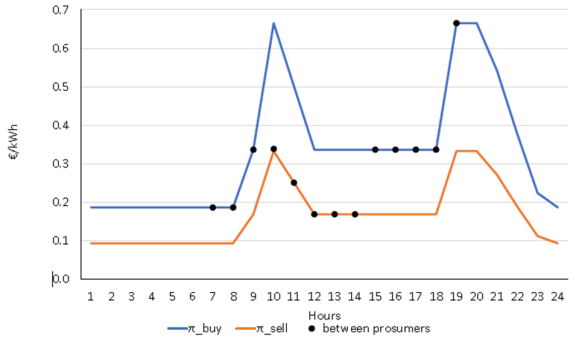

Fig. 4. Profile of prices π_{buy} and π_{sell}. Dots represent the energy prices of the exchanges between prosumers for the base case operating condition.

Fig. 4 also shows the prices of the internal transactions, when present. Since the model contains integer variables due to the modulus in constraint (15) and Gurobi provides the dual values only for continuous models, the solution is repeated without constraint (15) and by fixing to zero P^+ or P^- according to the first solution. As expected, the solutions of the continuous and mixed integer models are the same.

For the base case scenario, we compare here the solutions of three models:

- the LEC model;
- the model in which internal transactions are forbidden, i.e., $P_{\text{grid}} = P$ for each *i* and *t*;
- the LEC model without transactions between prosumers

connected to different feeders (separated feeders), i.e., constraint (16) is replaced by

$$P_{\text{grid\_in}\,k,t} = P_{\text{in}\,k,t} \tag{17}$$

for each branch k connected to the substation.

The comparison between the value of objective (1), the objective augmented with the weighted penalization of network and battery losses, the value of power loss in the network inside the community, and the computational time is shown in TABLE III. The LEC allows for a reduction of the total procurement cost and also reduces the power loss in the internal network. The LEC model that couples all the feeders achieves the lowest total costs. The computational time is low, and the optimal solution is always obtained with the default values of Gurobi parameters.

TABLE III COMPARISON BETWEEN THE SOLUTIONS FOR THE BASE CASE.

	OF (thousand euros)	Augmented *OF*	Losses (MWh)	CPU time (s)
LEC	45.7	45.7 10^3	3.19	9.9
without internal transaction	49.2	49.2 10^3	3.48	4.9
LEC separated feeders	47.1	47.1 10^3	3.34	6.51

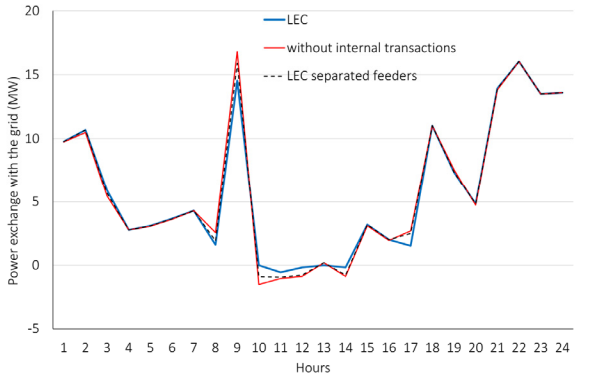

Fig. 5. Comparison between the profiles of the power flow exchanged with the utility grid (positive if consumed by the LEC) given by the LEC model, the model without internal transactions, and the LEC model without transactions between different feeders for the base case.

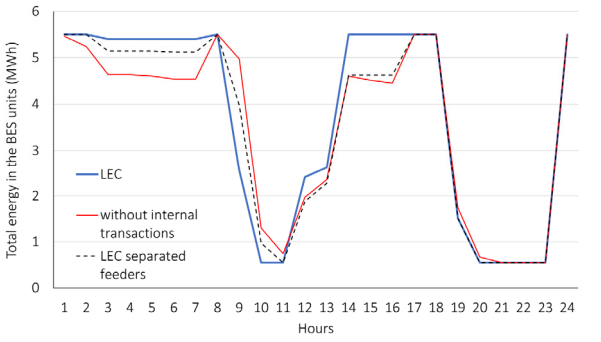

Fig. 6. Comparison between the profile of the total energy in the batteries of the LEC given by the three considered models for the base case.

Fig. 5 shows the comparison between the power exchanges with the utility grid for the three considered solutions. Fig. 6 shows the comparison between the profiles of the total energy in the BES units inside the community. Fig. 7 and Fig. 8 show, for each time interval, the total injection by the users that acts as producers and the total consumption of the consumers, respectively. Moreover, Fig. 7 shows the profile of the energy directly sold by the producers to other LEC participants.

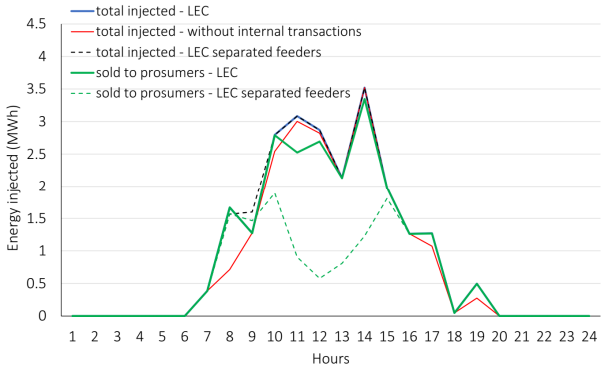

Fig. 7. Comparison between the profiles of the total energy injected in the LEC network by the producers in the base case. Comparison between the profiles of the energy directly sold to other LEC participants.

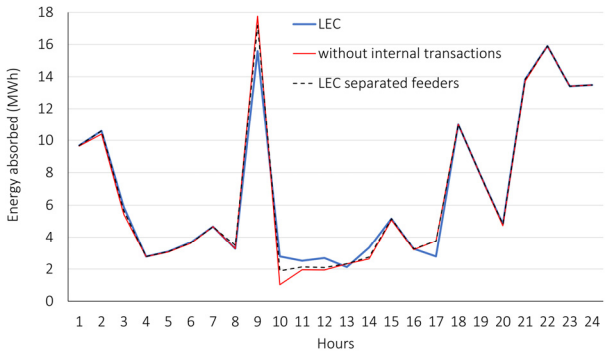

Fig. 8. Comparison between the profiles of the total energy consumed by the users in the LEC in the base case.

TABLE IV ENERGY PROCUREMENT COSTS IN THE THOUSANDS OF EUROS FOR EACH PROSUMER: BASE CASE.

prosumer	feeder	LEC	without internal transactions	LEC separated feeders
1	a	4.20	4.56	4.20
2	a	6.54	6.91	6.54
3	a	1.47	1.80	1.47
4	a	0.77	1.34	0.78
5	a	3.05	3.07	3.05
6	b	8.82	9.30	9.30
7	b	8.12	8.56	8.54
8	b	6.96	7.36	7.36
9	c	0.48	0.69	0.64
10	c	0.44	0.49	0.47
11	c	1.36	1.37	1.24
12	c	1.16	1.37	1.18
13	c	2.33	2.34	2.30

Each of the prosumers receives a benefit from the participation in the LEC, as shown by TABLE IV. Indeed, the total costs for each prosumer calculated with the LEC model are lower than the corresponding costs calculated without direct transactions between prosumers. The results are obtained by allocating the losses in each feeder to the prosumers connected to the same feeder proportionally to the power injection or consumption.

Comparing the results for the LEC with separated feeder with those of the LEC model that allows transactions between different feeders, some of the prosumers have reduced costs and some increased costs. The prosumers connected to feeder b obtain increased costs in the model with three separate feeders since none of them is equipped with PV units, although some advantage in the participation in the LEC could be achieved due to presence of the batteries.

B. Case with increased PV production and storage

With respect to the base case, both the PV productions and the battery sizes are doubled so the total daily PV production is 112 MWh (57.4% of the load) and the total capacity of the BES units is 11 MWh. Fig. 9 shows the prices of the internal transactions obtained by the solution of the LEC model.

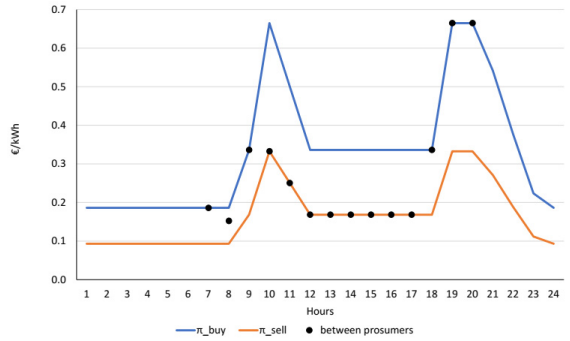

Fig. 9. Comparison between the energy prices of the transactions between prosumers (dots) and the profiles of prices π_{buy} and π_{sell} for the case with increased PV production.

TABLE V shows the values of objective (1), of the objective augmented with the weighted penalization of network and battery losses, of the value of power loss in the network inside the community, and of the computational time for the three models. Similar conclusions of the base case apply.

TABLE V COMPARISON BETWEEN THE SOLUTIONS FOR THE CASE WITH INCREASED PV PRODUCTION.

	OF (thousand euros)	Augmented *OF*	Losses (MWh)	CPU time (s)
LEC	29.4	29.4 10^3	5.39	7.59
without internal transactions	34.4	34.4 10^3	5.87	5.24
LEC separated feeders	31.9	31.9 10^3	6.25	6.20

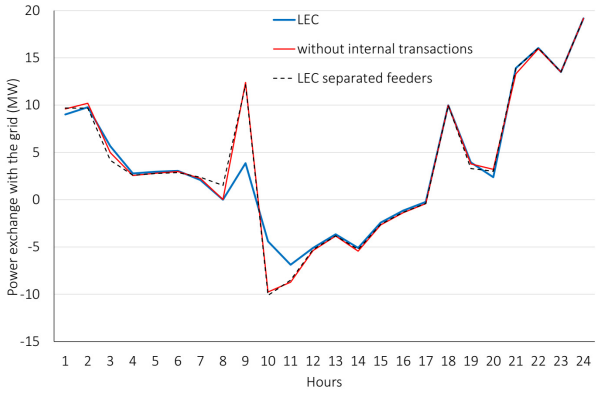

Fig. 10. Comparison between the profiles of the power flow exchanged with the utility grid in the case with increased PV production.

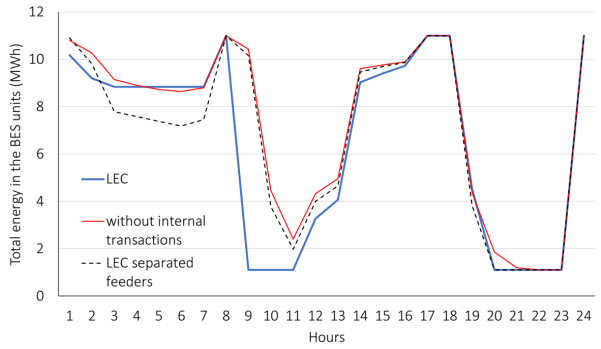

Fig. 11. Comparison between the profiles of the total energy in the batteries of the LEC in the case with increased PV production.

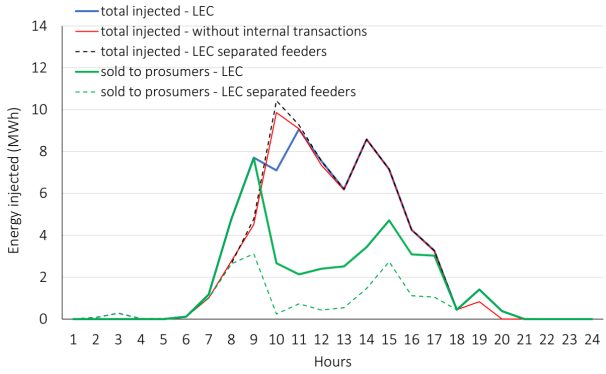

Fig. 12. Profiles of the total energy injected in the LEC network by the producers and of the energy directly sold to other LEC participants in the case with increased PV production.

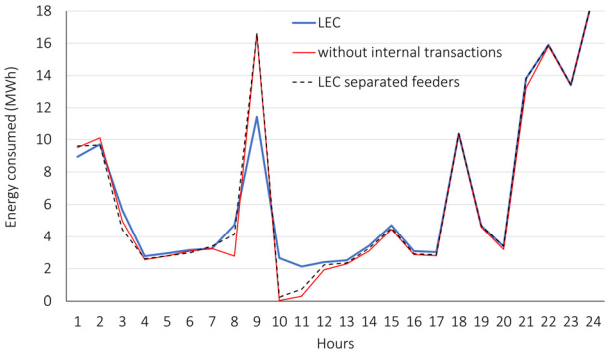

Fig. 13. Comparison between the profiles of the total energy absorbed by the consumers in the case with increased PV production.

Fig. 10, Fig. 11, Fig. 12, and Fig. 13 show the comparison between the power exchanges with the utility grid, the profiles of the total energy in the BES units inside the community, the total injection by the producers, and the total consumption of the consumers, respectively. Fig. 12 also shows the profile of the energy directly sold by the producers to other LEC participants.

As shown in TABLE VI, none of the prosumers is economically penalized by the participation in the LEC. The users connected to feeder b obtain a significant advantage from the participation in the LEC only if the transactions between different feeders are allowed, because of the lack of PV production.

TABLE VI ENERGY PROCUREMENT COST IN THE THOUSANDS OF EUROS (NEGATIVE VALUES INDICATE REVENUES) FOR EACH PROSUMER: INCREASED PV PRODUCTION.

prosumer	feeder	LEC	without internal transactions	LEC separated feeders
1	a	3.42	4.03	3.41
2	a	5.34	5.93	5.33
3	a	-0.82	-0.42	-0.80
4	a	-3.74	-3.08	-3.72
5	a	2.46	2.46	2.45
6	b	8.09	8.92	8.91
7	b	7.65	8.33	8.31
8	b	6.29	6.99	6.99
9	c	-0.84	-0.61	-0.68
10	c	-0.78	-0.61	-0.72
11	c	0.39	0.43	0.41
12	c	0.39	0.47	0.46
13	c	1.60	1.60	1.59

IV. CONCLUSIONS

The paper presents an optimization model for the day-ahead scheduling of the prosumers in a local energy community that allows direct transactions between participants. The model considers the main operational constraints and the losses. By reducing the total procurement costs of the LEC, the model gives priority to the use of internal energy resources. Moreover, the model provides the price of each direct transaction inside the LEC so that the costs and revenues of each prosumer are defined. This results in an important practical aspect: the model guarantees that none of the prosumers is economically penalized by the participation in the LEC.

The model presents a decomposable structure that appears appropriate for the implementation of a distributed optimization strategy.

The properties of the model are illustrated for a test network with three feeders in which the exchanges between the prosumers connected in different feeders are permitted.

The results show that the model finds the optimal solution with a low computational effort. The model also provides an indication of the optimal prices of the transactions between prosumers of the LEC. The comparison between the results obtained with the same model with and without the possibility of direct transactions among the prosumers show that each prosumer has an advantage by the participation in the community without cross-subsidization between active and non-active customers.

ACKNOWLEDGMENT

The authors thank Prof. Carlo Alberto Nucci for helpful discussions during the development of this work.

REFERENCES

[1] V. Heinisch, M. Odenberger, L. Göransson, and F. Johnsson, "Organizing prosumers into electricity trading communities: Costs to attain electricity transfer limitations and self-sufficiency goals," *Int. J. Energy Res.*, vol. 43, no. 13, pp. 7021–7039, 2019, doi: 10.1002/er.4720.

[2] H. Wang, N. Good, P. Mancarella, and K. Lintern, "PV-battery community energy systems: Economic, energy independence and network deferral analysis," in *International Conference on the European Energy Market, EEM*, 2017, no. November, doi: 10.1109/EEM.2017.7982021.

[3] D. Vangulick, B. Cornelusse, and D. Ernst, "Blockchain for peer-to-peer energy exchanges: Design and recommendations," *20th Power Syst. Comput. Conf. PSCC 2018*, pp. 1–7, 2018, doi: 10.23919/PSCC.2018.8443042.

[4] S. Wang, A. F. Taha, J. Wang, K. Kvaternik, and A. Hahn, "Energy crowdsourcing and peer-to-peer energy trading in blockchain-enabled smart grids," *IEEE Trans. Syst. Man, Cybern. Syst.*, vol. 49, no. 8, pp. 1612–1623, 2019, doi: 10.1109/TSMC.2019.2916565.

[5] G. van Leeuwen, T. AlSkaif, M. Gibescu, and W. van Sark, "An integrated blockchain-based energy management platform with bilateral trading for microgrid communities," *Appl. Energy*, vol. 263, no. October 2019, p. 114613, 2020, doi: 10.1016/j.apenergy.2020.114613.

[6] B. Yan, M. Di Somma, P. B. Luh, and G. Graditi, "Operation optimization of multiple distributed energy systems in an energy community," *Proc. - 2018 IEEE Int. Conf. Environ. Electr. Eng. 2018 IEEE Ind. Commer. Power Syst. Eur. EEEIC/I CPS Eur. 2018*, 2018, doi: 10.1109/EEEIC.2018.8494476.

[7] I. F. G. Reis, M. A. R. Lopes, and C. H. Antunes, "Energy transactions between energy community members: An agent-based modeling approach," *2018 Int. Conf. Smart Energy Syst. Technol. SEST 2018 - Proc.*, 2018, doi: 10.1109/SEST.2018.8495635.

[8] L. Han, T. Morstyn, C. Crozier, and M. McCulloch, "Improving the scalability of a prosumer cooperative game with K-means clustering," *2019 IEEE Milan PowerTech, PowerTech 2019*, pp. 1–6, 2019, doi: 10.1109/PTC.2019.8810558.

[9] F. Moret and P. Pinson, "Energy collectives: a community and fairness based approach to future electricity markets," *IEEE Trans. Power Syst.*, vol. 34, no. 5, pp. 3994–4004, 2019, doi: 10.1109/TPWRS.2018.2808961.

[10] R. Madani, M. Ashraphijuo, and J. Lavaei, "Promises of conic relaxation for contingency-constrained optimal power flow problem," *2014 52nd Annu. Allert. Conf. Commun. Control. Comput. Allert. 2014*, vol. 31, no. 2, pp. 1064–1071, 2014, doi: 10.1109/ALLERTON.2014.7028573.

[11] L. Gan, N. Li, U. Topcu, and S. H. Low, "Exact convex relaxation of optimal power flow in radial networks," *IEEE Trans. Automat. Contr.*, vol. 60, no. 1, pp. 72–87, 2015, doi: 10.1109/TAC.2014.2332712.

[12] W. Wei, J. Wang, N. Li, and S. Mei, "Optimal power flow of radial networks and its variations: a sequential convex optimization approach," *IEEE Trans. Smart Grid*, vol. 8, no. 6, pp. 2974–2987, 2017, doi: 10.1109/TSG.2017.2684183.

[13] S. H. Low, "Convex relaxation of optimal power flow - Part i: Formulations and equivalence," *IEEE Trans. Control Netw. Syst.*, vol. 1, no. 1, pp. 15–27, 2014, doi: 10.1109/TCNS.2014.2309732.

[14] S. H. Low, "Convex relaxation of optimal power flow-part II: Exactness," *IEEE Trans. Control Netw. Syst.*, vol. 1, no. 2, pp. 177–189, 2014, doi: 10.1109/TCNS.2014.2323634.

[15] D. K. Molzahn and I. A. Hiskens, "Convex relaxations of optimal power flow problems: an illustrative example," *IEEE Trans. Circuits Syst. I Regul. Pap.*, vol. 63, no. 5, pp. 650–660, 2016, doi: 10.1109/TCSI.2016.2529281.

[16] S. Lilla, C. Orozco, A. Borghetti, F. Napolitano, and F. Tossani, "Day-Ahead Scheduling of a Local Energy Community: An Alternating Direction Method of Multipliers Approach," *IEEE Trans. Power Syst.*, vol. 35, no. 2, pp. 1132–1142, Mar. 2020, doi: 10.1109/TPWRS.2019.2944541.

[17] M. E. Baran and F. F. Wu, "Optimal sizing of capacitors placed on a radial distribution system," *IEEE Trans. Power Deliv.*, vol. 4, no. 1, pp. 735–743, 1989, doi: 10.1109/61.19266.

[18] S. Cinvalar, J. J. Grainger, H. Yin, and S. S. H. Lee, "Distribution feeder reconfiguration for loss reduction," *IEEE Trans. Power Deliv.*, vol. 3, no. 3, pp. 1217–1223, 1988, doi: 10.1109/61.193906.